





Cite this: *New J. Chem.*, 2023, 47, 11525

Dehydration mechanism of fructose to 5-hydroxymethylfurfural catalyzed by functionalized ionic liquids: a density functional theory study†

Jiehao Hu,^a Mengting Yu,^a *^a Yao Li,^b Xiaoli Shen,^a Shenyu Cheng,^a Tianyou Xu,^a Chengsheng Ge,^a Yihang Yu^a and Zhaoyang Ju *^a

Ionic liquids (ILs) have shown great catalytic effects in the conversion of fructose to 5-hydroxymethylfurfural (HMF) but the dehydration mechanism remains ambiguous. In this work, density functional theory (DFT) calculations have been carried out for the mechanism of the dehydration of fructose to HMF, catalyzed by functionalized ILs. ILs with different kinds of functionalized imidazolium-based cations and SO₃ group-based anions have been used to investigate the catalytic effects of different anions and cations on the dehydration of fructose. The whole reaction process of fructose to HMF includes three dehydration steps. The overall rate-determining step is the second dehydration, and the functionalized cations showed good proton transfer ability to catalyze the reaction in the dehydration steps. The proton shuttling ability of cations is better than that of anions. The anions can form strong H-bonds with the fructose and cations and provide a polar environment to stabilize intermediates and transition states. The high catalytic activity is attributed to the synergetic catalysis of cations and anions to complete the dehydration of fructose. The dehydration reaction mechanism from fructose to HMF catalyzed by [BmimHSO₃][HSO₄]-functionalized ILs has been proposed by DFT calculations. This study emphasizes the catalytic performance of functionalized ILs replaced by different substituent groups and the dehydration mechanism of fructose to HMF.

Received 19th March 2023,
Accepted 19th May 2023

DOI: 10.1039/d3nj01286g

rsc.li/njc

Introduction

In recent years, renewable energy and green sources have been rapidly developed to face the global challenges of energy and environmental crises.^{1,2} The conversion of biomass into high-value-added chemicals and biofuels has become a good developing trend. As a critical raw material for the synthesis of platform chemicals, 5-hydroxymethylfurfural (HMF) has been widely used to produce levulinic acid, 2,5-dimethylfuran, 5-hydroxymethylfuroic acid, and 2,5-furandicarboxaldehyde.^{3,4} HMF can also be used to synthesize 2,5-furandicarboxylic acid, which is a promising monomer for the manufacture of bio-based polyethylene furanate to replace the petroleum-based polyethylene terephthalate.^{5,6}

For the production of HMF, various catalysts have been developed such as homogeneous and heterogeneous catalysts.^{7,8} As a new kind of highly efficient green media, ionic liquids (ILs)

have gained rapid development in recent years.^{9,10} On account of their unique physicochemical properties, such as high thermal stability, ultralow volatility, low melting points, and good ability to dissolve various substances,¹¹ ILs have provided a new opportunity for the efficient and clean manufacture of HMF from biomass. In the past decades, a series of ILs have been devoted to the synthesis of HMF from sugars.¹² Using ILs as the solvent and catalyst, Moreau *et al.*¹³ showed an efficient conversion of fructose and sucrose by 1-*H*-3-methylimidazolium chloride (HmimCl), giving a yield of HMF near 92%. In addition, ILs in conjunction with Lewis acidic catalysts, such as AlCl₃ and CrCl₃, can increase the dehydration of fructose by coordinating with the anions of ILs.^{14,15} Brønsted acid ILs, including sulfonic acid-functionalized ILs, can also be used for the effective conversion of fructose. The intra- and inter-molecular H-bonds coexist in the sulfonic acid-functionalized ILs, and they play an important role in the stability of the system.¹⁶ Kraus *et al.*¹⁷ reported a series of sulfonic acid-functionalized ILs that can effectively convert fructose to 5-alkoxymethylfurfural ethers and the functionalized ILs play a crucial role in the system, not only as a catalyst but also as a reaction medium to solubilize fructose. In the same year, Sim *et al.*¹⁸ proposed that bis-sulfonic acid ILs can efficiently convert fructose to HMF in 75% isolated yield, which was a 10% increment as compared to the mono-sulfonic acid ILs.

^a College of Chemical & Material Engineering, Quzhou University, Quzhou, China.
E-mail: 39090@qzc.edu.cn, jzy@qzc.edu.cn

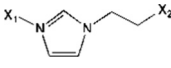
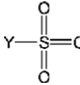
^b Beijing Key Laboratory of Ionic Liquids Clean Process, State Key Laboratory of Multiphase Complex Systems, Institute of Process Engineering, Chinese Academy of Sciences, Beijing, China

† Electronic supplementary information (ESI) available. See DOI: <https://doi.org/10.1039/d3nj01286g>

The application of ILs can enhance the selectivity of HMF and the conversion ratio. To obtain some basic aids to design more efficient ILs, the microscopic interaction mechanism between ILs and fructose was investigated.^{19–21} In our previous study, 25 different kinds of imidazolium-based ILs have been used for the interaction with fructose, H-bonds and π -stacking are the dominant driving forces for dissolving fructose in ILs.²² Guan *et al.*²³ reported the reaction mechanism for the conversion of glucose to HMF catalyzed by metal chlorides in 1-butyl-3-methylimidazolium chloride ILs by density functional theory (DFT) calculations and the metal centers exerted significant influences on the stabilities of the intermediates. For the conversion mechanism of glucose to HMF, there are two possible pathways, namely, the formation of a fructose intermediate and direct formation from 1,2-enediol species.²⁴ Caratzoulas *et al.*²⁵ reported the acid-catalyzed dehydration pathway from fructose to HMF, and three water molecules are formed. It is generally recognized that the catalytic conversion of cellulose to HMF proceeds through a tandem pathway (Scheme 1) including the hydrolysis of cellulose to glucose (step I), the isomerization of glucose to fructose (step II), and the dehydration of fructose to HMF (step III).^{24,26} Studying the reaction mechanism of the conversion of fructose is an important basis for understanding the utilization of sugars to biofuels and bioproducts. However, there is still the need for theoretical investigations of the dehydration mechanism of fructose catalyzed by functionalized ILs.

To study the effects of anion and cation structures on the conversion of fructose to HMF, a series of ILs (Table 1) including functionalized imidazolium-based cations (C1–C5) and sulfonic group-based anions (A1–A5) were calculated for the dehydration of fructose, due to the good ability of partially functionalized ILs in the dehydration of fructose reported by previous experiments.^{17,18} Herein, we have studied the catalytic effects on the dehydration of cation structures by changing the –OH, –COOH, –HSO₃ functional groups (C2–C4), the length of the alkyl chain (C4, C5), and the different functional groups in anions when the electronegativity of Y is changed by changing it to Cl, CF₃, CH₃, OH and methyl-benzene (*p*-CH₃C₆H₄) (A1–A5). We have mainly investigated the electronegativity of anions and cations replaced by different functional groups. The dehydration pathways catalyzed by different anions and cations were also probed by using DFT calculations. We mainly

Table 1 Structures of ILs used in this work

	C1	X ₁ = CH ₃	X ₂ = CH ₃
	C2	X ₁ = CH ₃	X ₂ = OH
	C3	X ₁ = CH ₃	X ₂ = COOH
	C4	X ₁ = CH ₃	X ₂ = HSO ₃
	C5	X ₁ = CH ₂ CH ₂ CH ₂ CH ₃	X ₂ = HSO ₃
	A1	Y = Cl	
	A2	Y = CF ₃	
	A3	Y = CH ₃	
	A4	Y = OH	
	A5	Y = <i>p</i> -CH ₃ C ₆ H ₄	

focus on the dehydration mechanism of fructose to HMF and the role of anions/cations of functionalized ILs. As a representative of Brønsted acidic ILs, [BmimHSO₃][HSO₄] was chosen to investigate the dehydration mechanism of fructose due to its wide use in biomass conversion. In addition, the reaction pathways catalyzed by the [BmimHSO₃][HSO₄] ionic pair are discussed. Finally, a novel reaction mechanism is proposed based on DFT calculations. This present study will provide basic aids for the design of efficient functionalized ILs catalysts, and for understanding the catalytic mechanism of the Brønsted acidic ILs in the transformation from fructose to HMF.

Computational method

In this work, the geometries of reactants, transition states (TSs), and products were optimized using the DFT method with the M06-2X-D3 hybrid exchange-correlation functional and the 6-311+G** basis set as implemented in the Gaussian 16 package;²⁷ the figures were generated by using the CYL view.²⁸ The Minnesota family of the M0X type density function was preferred as a general DFT method for describing nonbonded interactions and can give reliable results for ILs.^{29,30} In the M06-2X-D3 method, the D3 term represents a dispersion correlation and has good descriptions for the intermolecular interactions.^{31,32} The vibrational frequencies of all the structures were calculated to verify whether the structures were stationary points (no imaginary frequency) or TSs (only one imaginary frequency). Furthermore, the intrinsic reaction coordinate (IRC) pathways³³ were traced by using the second-order González-Schlegel integration method³⁴ to check the relative saddle points connecting each TS to the reactant and product. All reported Gibbs free energies, which were corrected by zero-point, had been calculated at the experimental temperature ($T = 298.15$ K and $P = 100$ kPa). The activation energy (G_a), which is the energy barrier, and reaction energy (G_r) of the systems are defined as follows:

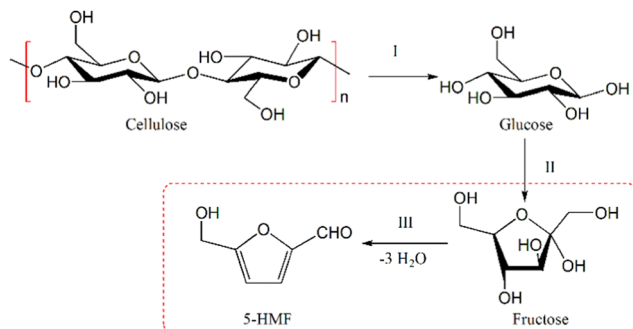
$$G_a = G_{TS} - G_R, G_r = G_P - G_R \quad (1)$$

where G_{TS} , G_R , and G_P represent the Gibbs free energies of the transition state, reactant, and product.

Results and discussion

Geometry properties of functionalized ionic liquids

It is of theoretical and practical significance to predict the reactive site of the molecular surface. Many prediction methods, such as



Scheme 1 The conversion of cellulose into glucose, fructose, and further to 5-hydroxymethylfurfural (HMF).

quantitative molecular surface analysis of electronic potential (ESP) and natural population analysis (NPA) charge, have been widely used based on the electrochemical structure of reactants.^{35–37} In a molecular system, the ESP can be defined as follows:

$$V_{\text{tot}}(r) = V_{\text{nuc}}(r) + V_{\text{ele}}(r) = \sum_A \frac{Z_A}{|r - R_A|} - \int \frac{\rho(r')}{|r - r'|} dr' \quad (2)$$

where Z and R are the nuclear charge and nuclear position, respectively, and $\rho(r)$ is the electronic density function of the molecule. The electronic potentials of the ESP surfaces, as well as the percentage area of sulfonic group-based anions and functionalized imidazolium-based cations, are given in Fig. 1 and Fig. S1 (SI†). As shown in Fig. 1, the highly positive and negative regions in the Y-SO_3 anions are around the Y and SO_3 groups, respectively. As shown in Fig. S1 (ESI†), taking ClSO_3^- as an example, the surface minimum of ESP (V_{min}) is -0.189 a.u., and the ESP of around -0.19 to -0.18 a.u. occupies a larger proportion of the total ESP area. There is only one peak value in the percentage of ESP surface area of ClSO_3^- and HSO_4^- . However, there is another peak value in the CF_3SO_3 , CH_3SO_3 , and $p\text{-CH}_3\text{C}_6\text{H}_4\text{SO}_3$ due to the electronegativity of substituents. For the cations ($X_1\text{-im-X}_2$), the most positive region is around the imidazolium ring. When X_2 is replaced by OH , COOH , and HSO_3 , it will have both electronegative and electropositive properties. For the BmimHSO_3^+ , the surface maximum of ESP (V_{max}) is 0.200 a.u., and the ESP of around $0.14\text{--}0.18$ a.u. occupies 62.2% of the total ESP area. The negative regions of fructose are around the hydroxyl and the electronegativity of the oxygen of the hydroxyl group is stronger than that of oxygen in the ring. The diverse substituents in ILs change

the physicochemical properties and will render different catalytic effects in the dehydration of fructose.

The dehydration of fructose to HMF

It's commonly accepted that the dehydration of fructose to HMF involves three dehydration processes as reported by previous studies.^{23,38} Firstly, the proton of C1 of fructose is transferred to the O2-H2 to finish the first dehydration. Then, the proton of O1 is transferred to the O3-H3 to complete the second dehydration. Finally, the proton of C5 transfers to O4-H4 to generate HMF. To compare the reaction barrier catalyzed by ILs of dehydration from fructose to HMF, we calculated the dehydration reaction of fructose without a catalyst. The computed mechanism details of fructose to HMF without catalysts are shown in Fig. 2. In the first dehydration step (R1-P1), the H of C1 is transferred to O2-H *via* TS1 with a barrier of $67.8 \text{ kcal mol}^{-1}$, resulting in C2–O2H bond cleavage. This step is calculated to be endothermic by $17.8 \text{ kcal mol}^{-1}$. Subsequently, R2 is converted to the P2 through TS2, where H of O1 is transferred to O3–H and releases another water molecule. The barrier of this process is calculated to be $37.3 \text{ kcal mol}^{-1}$. The transformation of R2 to P2 is calculated to be exothermic by $2.7 \text{ kcal mol}^{-1}$. Finally, the H of C5 is transferred to O4–H *via* TS3 with a barrier of $59.3 \text{ kcal mol}^{-1}$, which is in contrast to the first two steps of dehydration. The corresponding dehydration mechanism of fructose to HMF is plotted in Scheme 2. The barrier of each basic step is relatively high without catalysts. Therefore, the overall rate-determining step is the first dehydration in the absence of Brønsted acidic ILs.

To investigate the effects of dehydration sequences on the energy barriers, the different dehydration sequences of fructose were calculated. Generally, the reaction pathways of fructose to

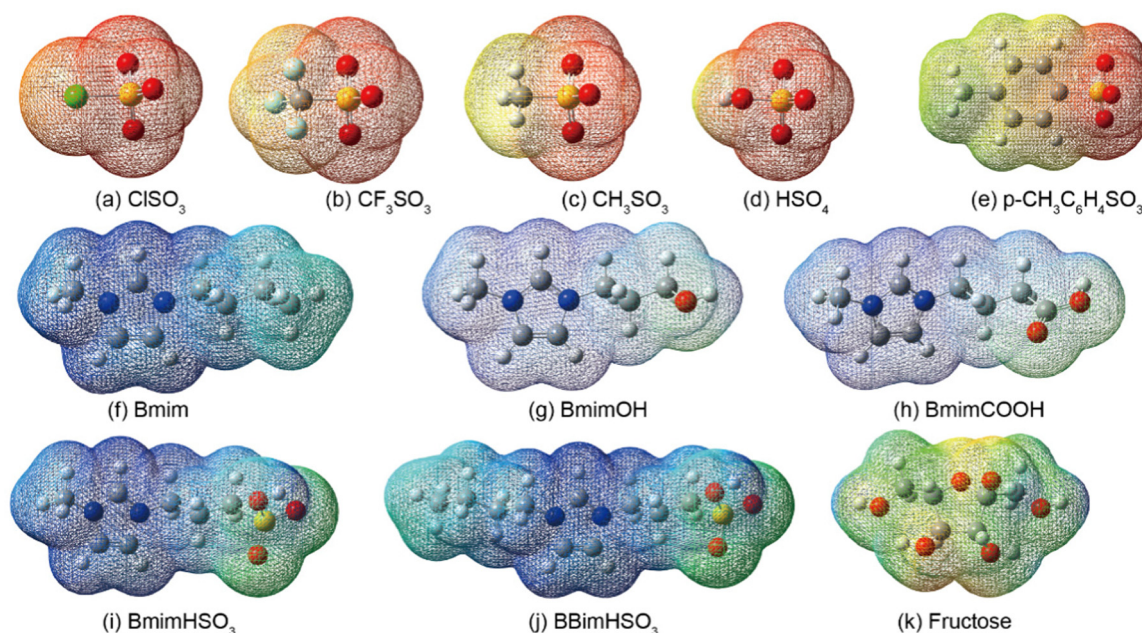


Fig. 1 The electrostatic potential surface of (a–e) anions, (f–j) cations, and (k) fructose. (Isovalue for the new surface: $\text{MO} = 0.02$ a.u.; density = 0.001 a.u.).

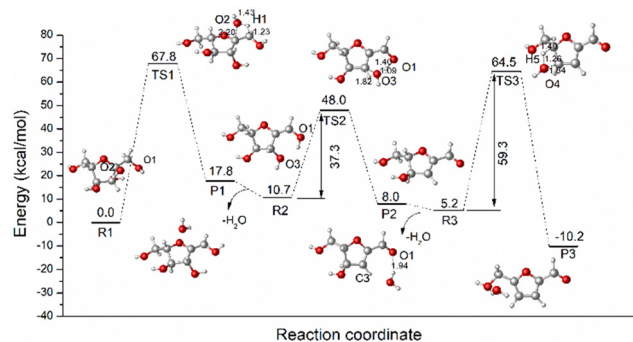
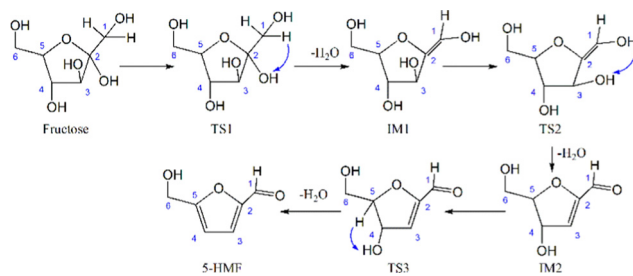


Fig. 2 Computed free energy profiles (energy kcal mol⁻¹) and optimized geometries of intermediates and TSs for the conversion of fructose to HMF without catalysts. (Bond distances in Å).



Scheme 2 The corresponding dehydration mechanism of fructose to HMF.

HMF have been reported by many studies *via* three steps of dehydration. For the first dehydration, the H of C1 will transfer to O2H2. Then, the H of O1H1 transfers to O2H2 to finish the second dehydration. Finally, the H of C5 transfers to O4H4 to finish the third dehydration.^{23,24} We named this dehydration pathway route 1-2-3. Here, we also probed the effects of different dehydration sequences, namely, routes 1-2-3, 1-3-2, 2-1-3, 2-3-1, 3-1-2, and 3-2-1. The corresponding energies and structures for when the second dehydration starts (H of C5 transfers to O4H4) are listed in Fig. S2 (ESI[†]). It was found that a four-membered ring was formed with an 89.2 kcal mol⁻¹ energy barrier, which was not consistent with the experiment. Therefore, the “second dehydration” should be followed by the “first dehydration”. Therefore, there are a total of 3 reaction pathways, which are route 1-2-3, 1-3-2, and 3-1-2, respectively. The energy barriers are summarized in Fig. S3 (ESI[†]). Route 1-2-3 will be more favorable with the lowest energy barrier, which is consistent with the acceptable dehydration mechanism reported before.^{23,24}

The Dehydration of fructose to HMF catalyzed by anions/cations

A series of studies on sulfonic acid-functionalized ILs have been successfully applied in fructose dehydration to HMF.^{17,39} Li *et al.* reported a theoretical explanation for the conversion mechanism of glucose to HMF catalyzed by 1-butyl-3-methylimidazolium chloride (C₄SO₃HmimCl) and they proposed that the cation plays a substantial role and mainly acts as a proton

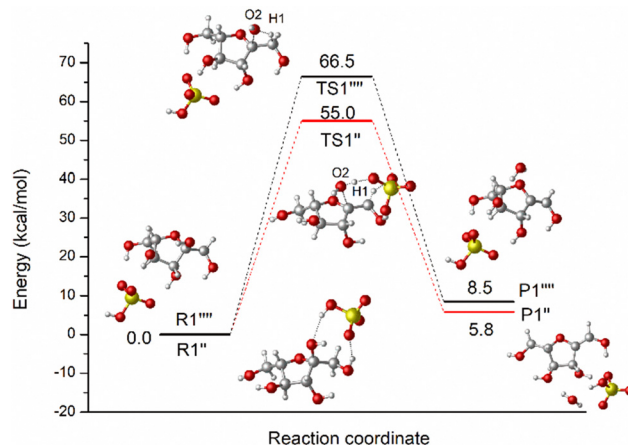


Fig. 3 Computed free energy profiles (energy kcal mol⁻¹) and optimized geometries of intermediates and TSs for the first dehydration catalyzed by HSO₄⁻ through different pathways.

shuttle to promote the reaction.³⁸ To investigate the catalytic mechanism by Brønsted acidic ILs, we used the first dehydration as an example; the dehydration mechanism catalyzed by HSO₄⁻ through two kinds of pathways is shown in Fig. 3. In the R1'''-P1''', H-bonds will be formed between HSO₄⁻ with the hydroxyl of fructose. A four-membered ring of C2, O2, H1, and C1 transition state will be formed with a 66.5 kcal mol⁻¹ energy barrier. In another reaction pathway (R1''-P1''), H1 transfers to the oxygen of HSO₄⁻ and the H of HSO₄⁻ transfers to the O2-H1 of fructose. An energy barrier of about 55.0 kcal mol⁻¹ is needed to finish this dehydration. Compared with the first dehydration without catalysts, the reaction barrier was reduced by 12.8 kcal mol⁻¹. The other two dehydrations catalyzed by HSO₄⁻ were also calculated and are listed in Fig. S4 and Fig. S5 (ESI[†]), respectively. There are two kinds of pathways to catalyze the dehydration by the HSO₄⁻, namely H-bonds formed between fructose and anions, and the proton shuttle through HSO₄⁻. From these three dehydration mechanisms of fructose catalyzed by HSO₄⁻, it can be concluded that the role of HSO₄⁻ mainly reflects on the proton transfer in the dehydration of fructose.

As an indispensable substance, water molecules also play an important role in the conversion of biofuel and bioproducts despite the main catalytic effects of anions and cations.⁴⁰ Based on the reaction barrier catalyzed by HSO₄⁻ above, it would be much better for the anions to go through the proton shuttle pathway as compared with the catalytic pathway *via* H-bonds formed between fructose and ILs. To compare the proton transfer ability of different catalysts, the energy profiles for the catalysis of fructose to HMF by HSO₄⁻, H₂O, and BmimHSO₃⁺ have been calculated and are presented in Fig. 4. The optimized geometries of the reactants, TSs, and intermediates for the catalysis of fructose to HMF by HSO₄⁻, H₂O, and BmimHSO₃⁺ are shown in Fig. 5 and Fig. 6, respectively. In the route from fructose to HMF catalyzed by H₂O (R-P), the H of C1 migrates to the O of H₂O and the H of H₂O migrates to the O2-H of fructose *via* TS1'. The energy barrier of the first degradation catalyzed by H₂O is 58.2 kcal mol⁻¹. The reaction is endothermic with a value

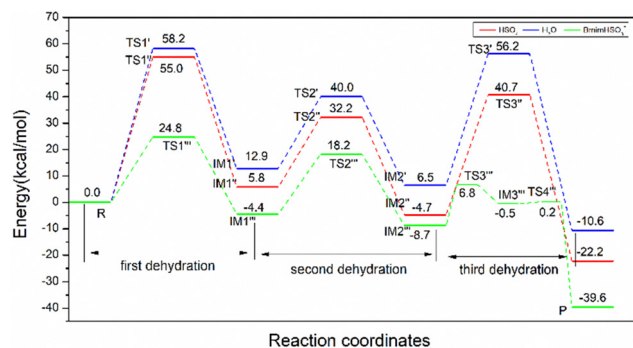


Fig. 4 Computed free energy profiles (energy kcal mol⁻¹) for the conversion of fructose to HMF, catalyzed by H₂O (R'-P'), HSO₄⁻ (R''-P''), and BmimHSO₃⁺ (R'''-P'''), which are plotted in red, blue and green, respectively.

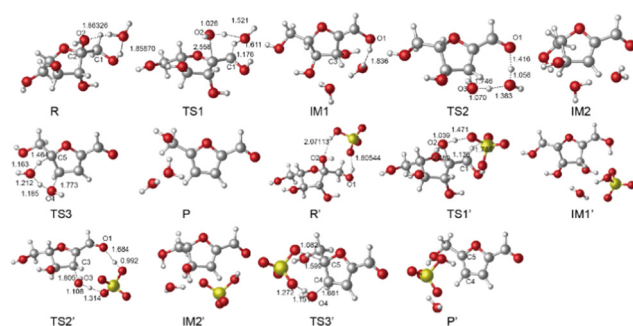


Fig. 5 Optimized geometries of the reactants, TSs, and intermediates in the reaction converting fructose to HMF, catalyzed by H₂O (R-P) and HSO₄⁻ (R'-P'). (Bond distances in Å)

of 12.9 kcal mol⁻¹. In the second dehydration, the H of O1 transfers to the O of H₂O, and the H of H₂O transfers to O3-H of IM1'. Subsequently, IM2' is formed *via* TS2' with an energy barrier of 27.1 kcal mol⁻¹. The reaction is exothermic by 6.4 kcal mol⁻¹. The H of C5 migrates to H₂O and the H of H₂O migrates to O4-H of IM2' *via* TS3'. The energy barrier in the third dehydration step is 49.7 kcal mol⁻¹. This reaction is exothermic with a value of 17.1 kcal mol⁻¹. The reaction pathways from fructose to HMF catalyzed by HSO₄⁻ are similar to H₂O; besides, the proton transfer ability of HSO₄⁻ is better than that of H₂O. The dehydration of fructose catalyzed by BmimHSO₃⁺ had also been probed by DFT calculations. The optimized geometries of the conversion of fructose to HMF catalyzed by BmimHSO₃⁺ are shown in Fig. 6. In the first two dehydration steps, the reaction pathways are similar to H₂O or HSO₄⁻, which is mainly reflected in the role of the proton shuttle. However, the energy barrier catalyzed by BmimHSO₃⁺ is lower than that of HSO₄⁻. In the third dehydration, there are two steps to finish the dehydration reaction. Firstly, the H of HSO₄⁻ transfers to O4-H with a 15.5 kcal mol⁻¹ energy barrier. Secondly, the H of C5 transfers to the cations easily with only a 0.7 kcal mol⁻¹ energy barrier. The order of different catalysts in transferring a proton is BmimHSO₃⁺ > HSO₄⁻ > H₂O. This is why sulfonic acid-functionalized ILs show good catalytic effects in the reaction.

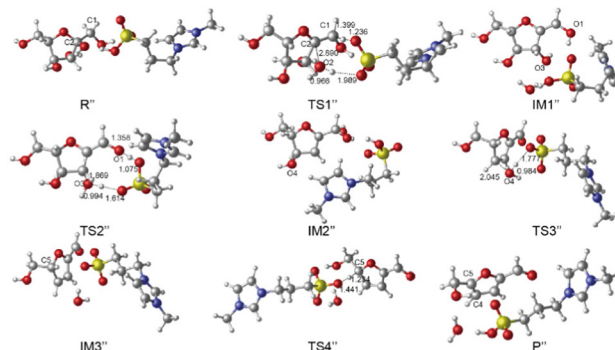


Fig. 6 Optimized geometries of the reactants, TSs, and intermediates in the reaction converting fructose to HMF, catalyzed by BmimHSO₃⁺ (R''-P''). (Bond distances in Å).

Table 2 Calculated activation energy (Ga) and reaction energy (Gr) for the first dehydration of fructose catalyzed by different anions and cations at the M06-2X-D3/6-311+G** level

Anions	Ga	Gr	Cations	Ga	Gr
ClSO ₃ ⁻	67.4	9.9	Bmim ⁺	67.3	10.3
CF ₃ SO ₃ ⁻	68.1	10.3	BmimOH ⁺	47.5	11.2
CH ₃ SO ₃ ⁻	66.2	9.2	BmimCOOH ⁺	35.7	2.9
HSO ₄ ⁻	55.0	5.8	BmimHSO ₃ ⁺	24.8	-4.4
<i>p</i> -CH ₃ C ₆ H ₄ SO ₃ ⁻	64.5	8.3	BBimHSO ₃ ⁺	24.6	2.7

Besides, experimental studies have shown that the catalytic activities of sulfonic acid-functionalized materials (C-SO₃H) for the conversion of fructose into HMF also follow the order of their acid strength.⁴¹

To investigate the catalytic effects of different anions and cations, taking the first dehydration of fructose, for example, the activation energies and reaction energies for the dehydration of fructose catalyzed by different anions and cations are shown in Table 2. Fig. 3 shows that in the first dehydration of fructose catalyzed by HSO₄⁻, there are two kinds of pathways, namely, proton shuttle (R1''-TS1''-P1'') and H-bonds formed with fructose (R2'''-TS1'''-P1''') due to the special structure of HSO₄⁻ with the OH. HSO₄⁻ showed good catalytic effects on the dehydration of fructose through proton shuttling. For the anions including ClSO₃, CF₃SO₃, CH₃SO₃, and *p*-CH₃C₆H₄SO₃, H-bonds can be formed with fructose to catalyze the dehydration and the barriers are 67.4, 68.1, 66.2, and 64.5 kcal mol⁻¹, respectively. Thus, the order of the catalytic effect of anions is *p*-CH₃C₆H₄SO₃ > CH₃SO₃ > ClSO₃ > CF₃SO₃. The yield of conversion fructose into HMF catalyzed by [BmimHSO₃]-[*p*-CH₃C₆H₄SO₃] is around 67%, which is better as compared to the other BmimHSO₃⁺-based ILs, and Sim *et al.* proposed that the acidity of various ILs is another important factor for the catalytic performance of ILs.¹⁸ To compare the catalytic effect of cations, the dehydration energies catalyzed by the cations (X₁-im-X₂) are also collected in Table 2. The barrier catalyzed by cations is lower as compared to the anions in the same dehydration step. Therefore, it further confirmed that cations play a critical role in the dehydration of fructose. The barriers of BmimOH⁺, BmimCOOH⁺, and BmimHSO₃⁺,

are 47.5, 35.7, and 24.8 kcal mol⁻¹, respectively, and the order for catalytic effects is BmimHSO₃⁺ > BmimCOOH⁺ > BmimOH⁺. Therefore, the proton transfer ability of BmimHSO₃⁺ is better than that of the other ILs. The lowest energies of the second dehydration catalyzed by isolated anions and cations were also calculated and are summarized in Table S1 (ESI[†]). As shown in Fig. S4 (ESI[†]), in the second dehydration of fructose catalyzed by HSO₄⁻, there are two pathways, namely, the proton shuttle (R2''-TS2''-P2'') and H-bonds formed with fructose (R2'''-TS2'''-P2'''). Compared with the energies for the second dehydration, it was also found that both HSO₄⁻ and BmimHSO₃⁺ have good proton transfer-ability in the catalysis of the dehydration of fructose. The negative value of the reaction energy means that the second dehydration is an exothermic process.

The dehydration of fructose to HMF catalyzed by ionic pairs

The isolated anions and cations are the threshold for studying the role the ILs system played in the dehydration of fructose. We investigated the catalytic pathways of ionic pairs in the dehydration mechanism of fructose to HMF. In previous reports, the synergistic effects of ILs play an important role in the utilization of biomass and very strong H-bonds can be formed between the anions and lignocellulose.^{42,43} As one of the most widely used Brønsted acidic ILs, [BmimHSO₃][HSO₄] has been generally applied in biomass conversion experiments to replace the traditional acidic catalyst in the industry.^{44,45} In this work, we mainly focus on the mechanism of fructose dehydration to HMF and provide some basic aids for designing more effective ILs for biofuels and bioproducts. To clarify how the anions and cations of [BmimHSO₃][HSO₄] catalyzed the dehydration of fructose, the two ways in which anions and cations take part in the second dehydration have been discussed. The computed free energy profiles and optimized structures are shown in Fig. 7. As a proton shuttle to promote dehydration, we probed the dehydration primarily through the anion (IMd'-IME') and cation (IMd-IME) of [BmimHSO₃][HSO₄]. For IMd-IME, the HSO₄⁻ anion mainly forms H-bonds to stabilize fructose and the cations. H1 is transferred to the

functional group of the cations, and the proton of BmimHSO₃⁺ is transferred to O2H2 to complete the dehydration. The barrier of IMd-IME is 22.0 kcal mol⁻¹. However, along another pathway for the proton shuttled by HSO₄⁻ (IMd'-IME'), the barrier is 24.8 kcal mol⁻¹. Therefore, the cations play a critical role with proton shuttling to catalyze the dehydration of fructose to HMF. In our previous study of the interactions between fructose and ILs, the strength of the H-bond formed between fructose and anions is stronger than that of cations.⁴⁶ Therefore, combined with these studies, it can be concluded that the synergistic effects of the anions and cations play important roles in the dehydration of fructose to HMF.

To investigate the dehydration mechanism of fructose to HMF catalyzed by functionalized ILs, we chose [BmimHSO₃][HSO₄] ILs as a research subject since it is the most typical and widely used in biofuel conversion.^{44,47} The reaction pathways catalyzed by [BmimHSO₃][HSO₄] have been calculated and are listed in Fig. 8. The mentioned coordinates of reactants, TS, and products in the dehydration of fructose to HMF are summarized in Table S2 (ESI[†]). Initially, the O2H2 of fructose was protonated and H-bonds were formed between [BmimHSO₃] and the O₂H₂ of the fructose to release H₂O. The C2 of fructose was then coordinated with the oxygen of the cation to form a less stable conformer IMb. H1 was transferred to the SO₃H group *via* TS_{b-c} with a total barrier of 27.4 kcal mol⁻¹ to complete the first dehydration. After that, in the second dehydration (IMd-IME), the H1 of the hydroxyl of fructose is transferred to the SO₃H group of the cation, and the proton of SO₃H is transferred to O3H3 with a barrier of 22.0 kcal mol⁻¹. The cations play a critical role in the dehydration through proton shuttling to catalyze the reaction. The anions form H-bonds with fructose and cations to provide a polar environment to stabilize the structures. Then, to finish the third dehydration (IMf-IMh), the O4H4 can be protonated by BmimHSO₃⁺ with an energy barrier of 21.5 kcal mol⁻¹. Finally, the H5 is transferred to the HSO₃ group of cations to generate HMF. The whole process is exothermic with -18.3 kcal mol⁻¹, which means the conversion of fructose to HMF is thermodynamically feasible. As shown in Fig. 8, the overall barrier for the second dehydration step is 30.1 kcal mol⁻¹ (difference between TSd-e and IMa); according to the energetic span model developed by Shaik *et al.*,⁴⁸ the second dehydration is rate-limiting in the catalysis of fructose to HMF by [BmimHSO₃][HSO₄]. Similar calculated results can be also found in a previous report by Guan *et al.*²³ The SO₃H group of the cations plays an important role in proton shuttling and the HSO₄⁻ anion plays an auxiliary role *via* H-bonds to stabilize intermediates and transition states. The synergistic effects of anions and cations are the main catalytic pathways that promote the conversion of fructose to HMF.

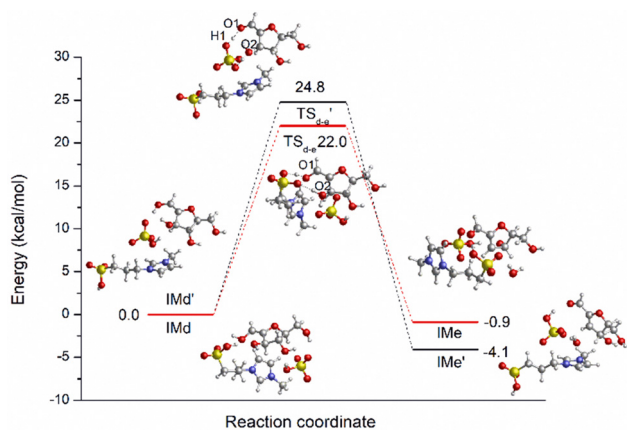


Fig. 7 Computed free energy profiles (energy kcal mol⁻¹) and optimized geometries of intermediates and TSs for the second dehydration catalyzed by [BmimHSO₃][HSO₄] through different pathways.

Conclusions

One of the most pressing challenges is the depleting supply of fossil fuels with the increasing energy demand. Biomass can be converted into platform chemicals such as sugars, furfural,

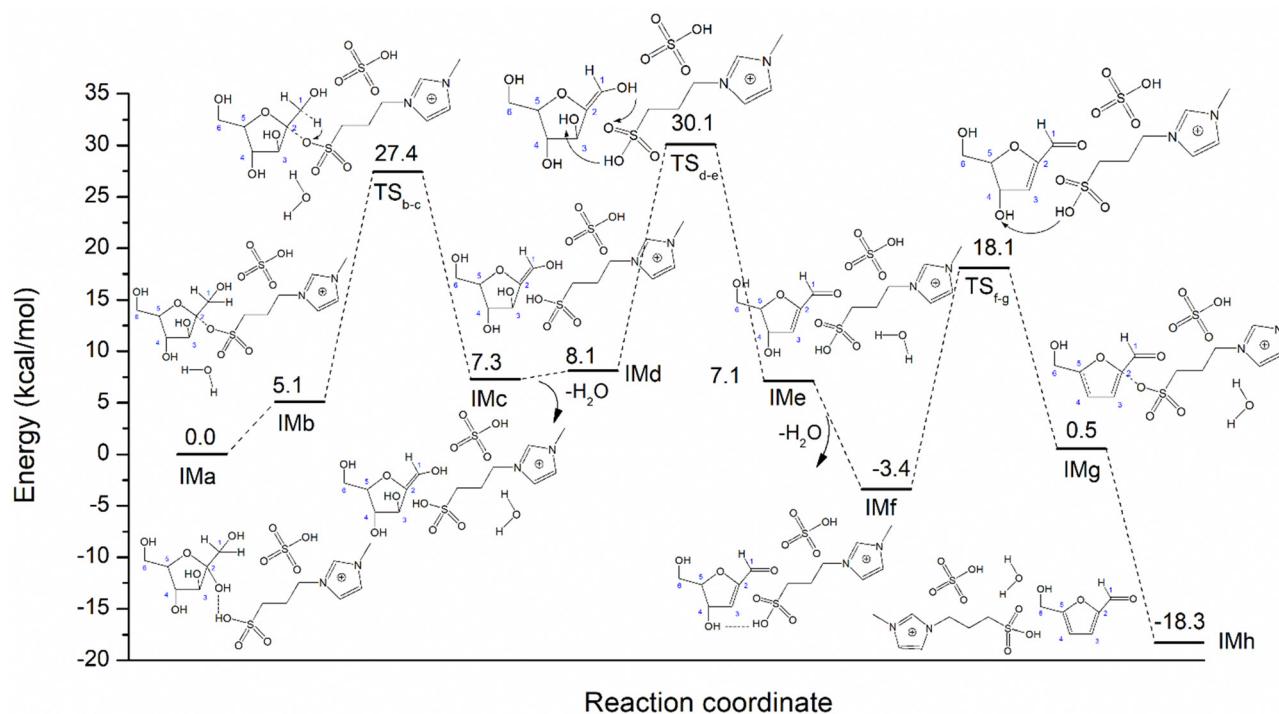


Fig. 8 Free energy profile and structures of the formation of HMF from fructose catalyzed by [BmimHSO₃][HSO₄].

levulinic acid, *etc.*, which can be further transformed into biofuels or other commodity chemicals. Fructose is one of the most widely studied types of biomass and its dehydration directly produces furfural. Functionalized ionic liquids (ILs) are classified as “green” solvents and these catalysts have been widely used in the dehydration of fructose to HMF. However, the mechanism for the dehydration of fructose to HMF, catalyzed by functionalized ILs, requires further study.

Based on DFT calculations, it can be concluded that there are three dehydration steps to be completed from fructose to HMF and the second dehydration step is the rate-determining step. In the dehydration step from fructose to HMF, the ILs catalysis is mainly reflected in the proton transfer ability; BmimHSO₃⁺ has a better transfer ability than H₂O or HSO₄[−] to catalyze the reaction. The anions can form strong H-bonds with fructose and cations and provide a polar environment to stabilize the intermediates and transition states. The synergistic effects of anions and cations play a critical role in the dehydration of fructose to HMF. The dehydration mechanism from fructose to HMF catalyzed by functionalized ILs was proposed by DFT calculations. The calculation data can provide further understanding, at the molecular level, of the reaction mechanism for the ionic liquid-promoted conversion of fructose to high-value-added biofuels.

Author contributions

Jiehao Hu: investigation and validation, Mengting Yu: methodology, investigation, supervision and writing – original draft. Yao Li: resources and writing – review & editing. Xiaoli Shen,

Shenyu Cheng, and Tianyou Xu: visualization and writing – review & editing. Chengsheng Ge: resources and project administration, Yihang Yu: validation and investigation. Zhaoyang Ju: conceptualization, funding acquisition and supervision.

Conflicts of interest

There are no conflicts to declare.

Acknowledgements

This research was financially supported by the Research Fund for the Program of “Xinmiao” (Potential) Talents in Zhejiang Province (No. 2022R435A002), Quzhou University (No. BSYJ202015 and BSYJ202113) and Lab Open Project (No. KFXM202204). The work was carried out at Shanxi Supercomputing Center of China, and the calculations were performed on TianHe-2.

References

- 1 L. T. Mika, E. Cséfalvay and Á. Németh, *Chem. Rev.*, 2018, **118**, 505–613.
- 2 J. Yan, O. Oyediji, J. H. Leal, B. S. Donohoe, T. A. Semelsberger, C. Li, A. N. Hoover, E. Webb, E. A. Bose, Y. Zeng, C. L. Williams, K. D. Schaller, N. Sun, A. E. Ray and D. Tanjore, *ACS Sustainable Chem. Eng.*, 2020, **8**, 8059–8085.
- 3 J. J. Bozell and G. R. Petersen, *Green Chem.*, 2010, **12**, 539–554.

- 4 R.-J. van Putten, J. C. van der Waal, E. de Jong, C. B. Rasrendra, H. J. Heeres and J. G. de Vries, *Chem. Rev.*, 2013, **113**, 1499–1597.
- 5 C. A. Antonyraj, N. T. T. Huynh, K. W. Lee, Y. J. Kim, S. Shin, J. S. Shin and J. K. Cho, *J. Chem. Sci.*, 2018, **130**, 156.
- 6 M. Konstantopoulou, Z. Terzopoulou, M. Nerantzaki, J. Tsagkalias, D. S. Achilias, D. N. Bikiaris, S. Exarhopoulos, D. G. Papageorgiou and G. Z. Papageorgiou, *Eur. Polym. J.*, 2017, **89**, 349–366.
- 7 Q. Hou, X. Qi, M. Zhen, H. Qian, Y. Nie, C. Bai, S. Zhang, X. Bai and M. Ju, *Green Chem.*, 2021, **23**, 119–231.
- 8 V. Tangsermvi, T. Pila, B. Boekfa, V. Somjit, W. Klysubun, J. Limtrakul, S. Horike and K. Kongpatpanich, *Small*, 2021, **17**, 2006541.
- 9 M. J. Trujillo-Rodríguez, H. Nan, M. Varona, M. N. Emaus, I. D. Souza and J. L. Anderson, *Anal. Chem.*, 2019, **91**, 505–531.
- 10 A. S. Amarasekara, *Chem. Rev.*, 2016, **116**, 6133–6183.
- 11 Z. Ju, W. Xiao, X. Yao, X. Tan, B. A. Simmons, K. L. Sale and N. Sun, *Phys. Chem. Chem. Phys.*, 2020, **22**, 2878–2886.
- 12 T. Ståhlberg, W. Fu, J. M. Woodley and A. Riisager, *ChemSusChem*, 2011, **4**, 451–458.
- 13 C. Moreau, A. Finiels and L. Vanoye, *J. Mol. Catal. A: Chem.*, 2006, **253**, 165–169.
- 14 Y. Yang, W. Liu, N. Wang, H. Wang, Z. Song and W. Li, *RSC Adv.*, 2015, **5**, 27805–27813.
- 15 Y. Yang, W. Liu, N. Wang, H. Wang, W. Li and Z. Song, *Chin. J. Chem.*, 2015, **33**, 583–588.
- 16 X.-M. Liu, Z.-X. Song and H.-J. Wang, *Struct. Chem.*, 2009, **20**, 509–515.
- 17 G. A. Kraus and T. Guney, *Green Chem.*, 2012, **14**, 1593–1596.
- 18 S. E. Sim, S. Kwon and S. Koo, *Molecules*, 2012, **17**, 12804–12811.
- 19 M. Dulski, A. Cecotka, S. N. Tripathy, A. Sakalowski, K. Wolnica, M. Tarnacka, R. Wrzalik, K. Kamiński and M. Paluch, *RSC Adv.*, 2016, **6**, 57634–57646.
- 20 J. Liu, F. Wang, Z. Li, J. Zhou, J. Chen and C. Xia, *Struct. Chem.*, 2011, **22**, 1119–1130.
- 21 A. H. Pakiari, S. Siahrostami and T. Ziegler, *J. Mol. Struct.: Theochem*, 2010, **955**, 47–52.
- 22 Z. Ju, X. Yao, Z. Luo, M. Cao and W. Xiao, *Carbohydr. Res.*, 2020, **487**, 107882.
- 23 J. Guan, Q. Cao, X. Guo and X. Mu, *Comput. Theor. Chem.*, 2011, **963**, 453–462.
- 24 J. Li, J. Li, D. Zhang and C. Liu, *J. Phys. Chem. B*, 2015, **119**, 13398–13406.
- 25 S. Caratzoulas and D. G. Vlachos, *Carbohydr. Res.*, 2011, **346**, 664–672.
- 26 Y. J. Pagán-Torres, T. Wang, J. M. R. Gallo, B. H. Shanks and J. A. Dumesic, *ACS Catal.*, 2012, **2**, 930–934.
- 27 M. J. Frisch, G. W. Trucks, H. B. Schlegel, G. E. Scuseria, M. A. Robb, J. R. Cheeseman, G. Scalmani, V. Barone, G. A. Petersson, H. Nakatsuji, X. Li, M. Caricato, A. V. Marenich, J. Bloino, B. G. Janesko, R. Gomperts, B. Mennucci, H. P. Hratchian, J. V. Ortiz, A. F. Izmaylov, J. L. Sonnenberg, D. Williams-Young, F. Ding, F. Lipparini, F. Egidi, J. Goings, B. Peng, A. Petrone, T. Henderson, D. Ranasinghe, V. G. Zakrzewski, J. Gao, N. Rega, G. Zheng, W. Liang, M. Hada, M. Ehara, K. Toyota, R. Fukuda, J. Hasegawa, M. Ishida, T. Nakajima, Y. Honda, O. Kitao, H. Nakai, T. Vreven, K. Throssell, J. A. Montgomery Jr, J. E. Peralta, F. Ogliaro, M. J. Bearpark, J. J. Heyd, E. N. Brothers, K. N. Kudin, V. N. Staroverov, T. A. Keith, R. Kobayashi, J. Normand, K. Raghavachari, A. P. Rendell, J. C. Burant, S. S. Iyengar, J. Tomasi, M. Cossi, J. M. Millam, M. Klene, C. Adamo, R. Cammi, J. W. Ochterski, R. L. Martin, K. Morokuma, O. Farkas, J. B. Foresman and D. J. Fox, *Gaussian*, Gaussian, Inc., Wallingford CT, 2016.
- 28 H. Guernon and C. Y. Legault, *Organometallics*, 2013, **32**, 1988–1994.
- 29 S. Zahn, D. R. MacFarlane and E. I. Izgorodina, *Phys. Chem. Chem. Phys.*, 2013, **15**, 13664–13675.
- 30 T. M. Simeon, M. A. Ratner and G. C. Schatz, *J. Phys. Chem. A*, 2013, **117**, 7918–7927.
- 31 S. Grimme, S. Ehrlich and L. Goerigk, *J. Comput. Chem.*, 2011, **32**, 1456–1465.
- 32 S. Grimme, J. Antony, S. Ehrlich and H. Krieg, *J. Chem. Phys.*, 2010, **132**, 154104.
- 33 K. Fukui, *J. Phys. Chem.*, 1970, **74**, 4161–4163.
- 34 C. Gonzalez and H. B. Schlegel, *J. Chem. Phys.*, 1991, **95**, 5853–5860.
- 35 R. Fu, T. Lu and F.-W. Chen, *Acta Phys.-Chim. Sin.*, 2014, **30**, 628–639.
- 36 F. Bulat, A. Toro-Labbé, T. Brinck, J. Murray and P. Politzer, *J. Mol. Model.*, 2010, **16**, 1679–1691.
- 37 Z. Wang, Y. Liu, B. Zheng, F. Zhou, Y. Jiao, Y. Liu, X. Ding and T. Lu, *J. Chem. Phys.*, 2018, **148**, 194106.
- 38 J. Li, J. Li, D. Zhang and C. Liu, *J. Phys. Chem. B*, 2015, **119**, 13398–13406.
- 39 S. E. Sim, S. Kwon and S. Koo, *Molecules*, 2012, **17**, 12804–12811.
- 40 K. Dong, X. Liu, H. Dong, X. Zhang and S. Zhang, *Chem. Rev.*, 2017, **117**, 6636–6695.
- 41 R. Liu, J. Chen, X. Huang, L. Chen, L. Ma and X. Li, *Green Chem.*, 2013, **15**, 2895.
- 42 Y. Li, X. Liu, S. Zhang, Y. Yao, X. Yao, J. Xu and X. Lu, *Phys. Chem. Chem. Phys.*, 2015, **17**, 17894–17905.
- 43 Y. Li, X. Liu, Y. Zhang, K. Jiang, J. Wang and S. Zhang, *ACS Sustainable Chem. Eng.*, 2017, **5**, 3417–3428.
- 44 H. Liu, X. Chen, Y. Zhang, M. Lu, H. Lyu, L. Han and W. Xiao, *Energy Fuels*, 2020, **34**, 7085–7093.
- 45 N. Gupta, Sonu, G. L. Kad and J. Singh, *Catal. Commun.*, 2007, **8**(9), 1323–1328.
- 46 Z. Ju, X. Yao, Z. Luo, M. Cao and W. Xiao, *Carbohydr. Res.*, 2020, **487**, 107882.
- 47 H. Li, Q. Zhang, X. Liu, F. Chang, Y. Zhang, W. Xue and S. Yang, *Bioresour. Technol.*, 2013, **144**, 21–27.
- 48 S. Kozuch and S. Shaik, *Acc. Chem. Res.*, 2011, **44**, 101–110.